Physics Letters A 376 (2012) 227–230

Contents lists available at SciVerse ScienceDirect

Physics Letters A

www.elsevier.com/locate/pla

Spike in transient photocurrent of organic solar cell: Exciton dissociation at interface

De-Li Li, Wei Si, Wen-Chao Yang, Yao Yao, Xiao-Yuan Hou, Chang-Qin Wu *

Department of Physics and State Key Laboratory of Surface Physics, Fudan University, Shanghai 200433, China

ARTICLE INFO

Article history:
Received 10 August 2011
Received in revised form 24 November 2011
Accepted 26 November 2011
Available online 30 November 2011
Communicated by R. Wu

Keywords:
Exciton dissociation
Transient photocurrent
Electrode/organic interface
Organic solar cell

ABSTRACT

The effect of exciton interfacial dissociation on transient photocurrent (TPC) in a single-layer organic solar cell is investigated within a time-dependent device model. The spike observed in TPC experiments is attributed to exciton dissociation at the electrode/organic interface. In comparison with the observed negative signal of transient photovoltage (TPV), the spike more directly reflects the charge processes at the interface. Moreover, numerical results show that the spike of TPC is sensitive to the voltage applied on the device and the hole mobility of the organic semiconductor. Further investigation on the spike by the favorable TPC technique is suggested to provide details about the exciton and carrier processes at the interface.

1. Introduction

With the introduction of bulk heterojunction structure, organic solar cells are proved to be promising candidates for low cost energy sources [1]. The dissociation of light-induced exciton at the various interfaces in these cells is identified as one of the essential processes for charge generation [2]. A comprehensive understanding of these processes is required to improve the efficiency. Recently, the transient photovoltage (TPV) techniques were applied to investigating some single layer organic solar cells. An abnormal polarity change from negative to positive was observed shortly after switching on the laser pulse [3–5]. The phenomenon was realized to be related to the exciton dissociation at the electrode/organic layer interface [6].

In comparison with TPV techniques, time-of-flight experiment (one of the transient photocurrent techniques) is used more frequently to measure the carrier's mobility [7]. Normally, the time-resolved signal exhibits an initial sharp spike followed by a wide platform until its decay. The mobility is obtained through determining the transit time t_{tr}, which denotes the moment at which the signal begins to decay [7–9]. TPC seems to be more sensitive to the charge carriers movements in the device. Thus, it is suggestive to investigate the effects of the exciton dissociation at the electrode/organic layer interface on the TPC.

Theoretically, the Monte Carlo method, which describes the dynamic processes of carriers in the bulk, has been adopted to simulate the TPC. The method treats the transit time as the average travel time of the photo-generated carrier from one electrode to the other [11]. However, the application of the Monte Carlo method is inconvenient, as the Poisson equation and role of the circuit must be treated carefully. Fortunately, the time-dependent device model provides a suitable means. Recently, we successfully extended the model and simulated the TPV signal. We obtained an excellent results compared with related experimental results [6]. In this Letter, this method is modified to investigate the interfacial effects on the TPC under the short-circuit condition.

2. Device model method

The model quantitatively addresses charge processes, exciton processes, the role of the contact interface and the evolution of the electric field by Poisson equation. The details of the model were presented in one of our previous works [6]. However, in order to simulate the transient photocurrent, some modification should be made because of its sensitivity to the circuit under such condition. To this end, we consider a model that contains a sensing resistor R connected in series to the organic layer. The voltage drop on the sensing resistor reflects the electric processes in the device. Similar with the treatment of Macdonald for one-dimensional current transport equation [12], the dynamic equation for $E(x)$ is given as

$$\frac{\partial}{\partial t}E(x,t) = \frac{1}{\varepsilon_0 \epsilon}\left[\frac{V_{\text{eff}}}{RS} - J(x,t)\right], \tag{1}$$

where ε_0 is the static dielectric constant, ϵ the relative permittivity, R the external resistor, S the area of the organic solar cell,

* Corresponding author.
E-mail address: cqw@fudan.edu.cn (C.-Q. Wu).

0375-9601/$ – see front matter
doi:10.1016/j.physleta.2011.11.055

$J(x,t)$ the current density in the device, and V_{eff} [$\equiv V_{\text{app}} - V_{\text{bi}} + \int_0^L E(x,t)\,dx$] the voltage drop on the organic device with V_{app} the applied voltage and V_{bi} the build-in voltage. Thus, the Poisson equation changes into a time-dependent equation of the electric field $E(x,t)$, in which both the effects of conduction current density $J(x,t)$ and displacement current density V_{eff}/RS are included. Besides, in the open-circuit condition, we simulate V_{eff}, which corresponds to the measured TPV. While near the short-circuit condition, the current transient, that goes through the external circuit, corresponds to the observed TPC. In the simulation, it is obtained by

$$I(t) = \frac{V_{\text{eff}}}{R}. \tag{2}$$

By including a resistance, the RC time constant should be treated carefully. During the TPC experiments, the load resistor R and the area of the cells are adjusted to ensure that the time constant RC of the circuit is at least 20 times shorter than the carrier transit time [10]. In our simulation, we set the load resistor R to be 50 Ω and a device area, 1 mm^2, which generate a time constant RC of about 5 ns. A time constant RC of 5 ns does not significantly influence the issues concerned in this Letter.

In the device we considered, excitons mainly dissociate at the interface, while some of them may dissociate in the bulk under the influence of defects and electric field [13,14]. Exciton dissociates at the interface mainly by injecting the electron into the electrode that works as an acceptor [2,5]. Although it is indicated that the dissociation is under sub-nanosecond, a detail knowledge of the process has not been achieved. In contrast, the process of exciton dissociation in the bulk is slow (microsecond) due to the absence of the donor/acceptor structure and of a high internal electric field. To address the issue, we define two dissociation rates, η_1 at the interface, where excitons undergo a fast dissociation within ~1 nm away from the anode [15], and η_2 in the bulk, which is assumed to be uniform across the device [14]. The exciton dynamic equation reads

$$\frac{\partial}{\partial t}\rho_{\text{ex}} - D\frac{\partial^2}{\partial x^2}\rho_{\text{ex}} = G(x,t) - \frac{\rho_{\text{ex}}}{\tau} - \eta(x)\rho_{\text{ex}}, \tag{3}$$

where ρ_{ex} is the density of excitons, D the diffusion constant, and $\eta(x) = \eta_1$ at the interface or η_2 in the bulk. The exciton generation function $G(x,t)$ follows the form of the input laser pulse in experiments, say,

$$G(x,t) = \begin{cases} G_0 \exp(-x/L_a), & t_{\text{on}} \leqslant t \leqslant t_{\text{off}}, \\ 0, & \text{otherwise}, \end{cases} \tag{4}$$

where G_0 is the generation rate of singlet excitons depending on the intensity of light, L_a the absorption length, and t_{on} ($\equiv 0$) and t_{off} the time when the laser is switched on and off, respectively. The boundary condition of the above equation is $\partial\rho_{\text{ex}}/\partial x = 0$.

3. Results and discussion

In the simulation, we take a single-layer device with the structure of ITO (indium tin oxide)/NPB (N,N-bis(l-naphthyl)-N,N-diphenyl-1,l-biphentl-4,4-diamine)/Al. The parameters are set as follows: the thickness of the device is 400 nm, the mobility of hole and electron $\mu_{\text{p}} = 1.0 \times 10^{-2}$ cm^2/Vs and $\mu_{\text{n}} = 5.0 \times 10^{-4}$ cm^2/Vs respectively, the lifetime of exciton 1 ns [13,16]. $G_0 = 1.0 \times 10^{-7}$ nm^{-3} ns^{-1} and the absorption length $L_a =$ 50 nm. The value of η_2 is several order smaller than that of η_1 due to the low exciton dissociation rate in the bulk [14]. We turn on the "laser pulse" at 0 ns and turn it off at 2 ns.

We first simulate the TPC response after switching on the laser pulse. A positive voltage of 1.0 V is applied to the ITO electrode

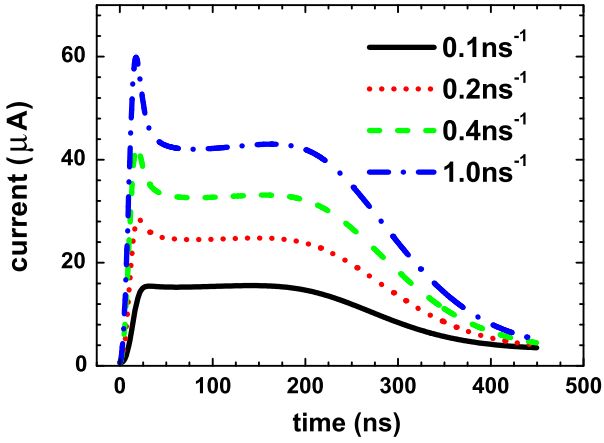

Fig. 1. The transient photocurrent for different exciton interfacial dissociation rates η_1 under a positive applied voltage of 1.0 V.

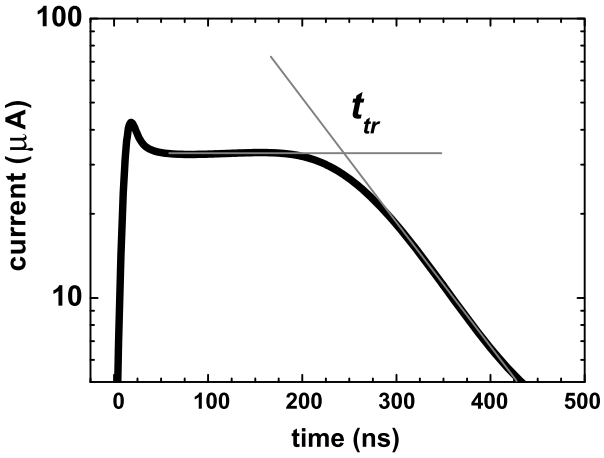

Fig. 2. The determination of the transit time t_{tr} by the intersect of the asymptotes in logarithm photocurrent versus time plots.

corresponding to the applied voltage of time-of-flight experiments in determining the charge carrier mobility. The exciton interfacial dissociation rate η_1 is varied, while η_2 is fixed at 1.0×10^3 s^{-1}. As can be seen in Fig. 1, TPC curve is obtained with an initial sharp spike followed by a wide platform, which qualitatively agrees with the experimental results [8–10]. In the standard time-of-flight experiment, the mobility is derived from the transit time denoted by the starting point of the decay of the TPC. The equation and its correction are $\mu = L^2/Vt_{\text{tr}}$ and $\triangle t_{\text{tr}}/t_{\text{tr}} = (2kT/eV)^{\frac{1}{2}}$ respectively, where k is the Boltzmann constant, T the temperature [17]. To verify our simulation results, Fig. 2 shows the transit time t_{tr} defined as the intersect of the asymptotes in logarithm photocurrent versus time plots for the case $\eta_1 = 0.4$ ns^{-1} [17]. The transit time given in Fig. 2 is the same as the one of about 260 ns derived from above equations.

As also can be seen in Fig. 1, the most significant effect is that the initial spike gets smaller when we decrease the exciton interfacial dissociation rate. Then, we changed η_2 by almost two orders of magnitude, while fix η_1. The simulated results is shown in Fig. 3. As illustrated, the magnitude of the TPC platform increases when η_2 rises. However, the initial spike is not sensitive to the exciton dissociation rate in the bulk. Thereupon we infer that the fast exciton interfacial dissociation rate induces an observable current spike that qualitatively agrees with the one observed in TPC experiments.

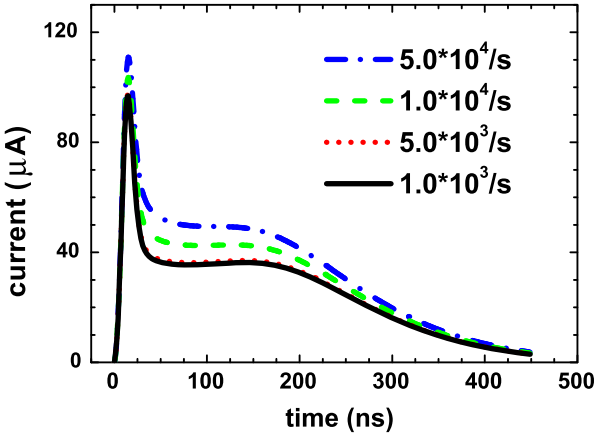

Fig. 3. The transient photocurrent for different bulk dissociation rates η_2 under a positive applied voltage of 1.0 V.

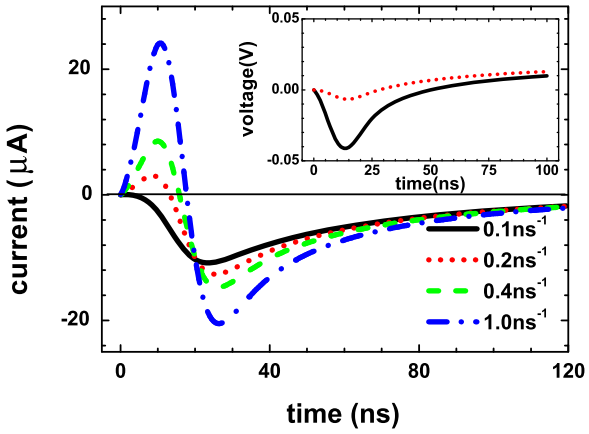

Fig. 4. The transient photocurrent for different exciton interfacial dissociation rates η_1 without applied voltage. The inset shows the TPV curve with $\eta_1 = 1.0$ ns^{-1} (the short dot line, red in the web version) and 1000.0 ns^{-1} (the black solid line) for comparison.

The origin of the spike is the same as the origin of the ultrafast negative signal of TPV [5,6]. Both of them are related with the exciton and charge carrier processes at the interface, which are more complicated than these in the bulk. Firstly, as mentioned above, the electrons and holes are separated by the interface during the exciton dissociation [2,5,13]. Secondly, the generated holes can diffuse into the bulk, drift under the electric field or recombine with the electrons in the anode. The diffusion and drift of the holes lead to a displacement of charges, which induces the observable TPV or TPC depending on the experiment conditions. Besides, the recombination takes away most of the generated holes and thus weakens the signals. From this model, no polarity change is expected for TPC when a positive voltage is applied, which is different from the TPV signals [5,6]. Under such condition, the holes, generated by exciton dissociation at the interface and in the bulk, transport to the other electrode under the internal electric field, which induces a transient current platform as shown in Fig. 1. The conduction current is in the same direction with the induced current by exciton dissociation at the interface.

The transient conductivity investigation on the subject offers the possibility of revealing the exciton and charge carrier physical processes at the interface as well as in the bulk. To compare with the case of TPV [5,6], we simulate the TPC of the above device without applied voltage. Under such condition, the build-in electric field drives the charge carriers towards the electrodes, which is the core of the mechanism of organic solar cells. Fig. 4 shows the simulation results, where we varied the exciton interfacial dissociate rate η_1 from 0.1 up to 1.0 ns^{-1}. The TPV curves, obtained under the open circuit condition with $\eta_1 = 1.0$ ns^{-1} and $\eta_1 = 1000.0$ ns^{-1} are also presented in the inset for comparison.

Focusing on Fig. 4, we find that the dependence of the spike on the interfacial dissociation rate is the same as that in Fig. 1. The inset shows the TPV curves with $\eta_1 = 1.0$ ns^{-1} and $\eta_1 = 1000.0$ ns^{-1}. The curves agree with the results of experiments very well, which further proves the relation of the negative signal with the exciton interfacial dissociation [5]. Another significant result is that TPC shows more transient characteristics by presenting a polarity change and a fast decay. The fast decay is absent in the TPV curves of the inset in Fig. 4. The fast decay of TPC is caused by the gradual extraction of charges by the electrode under a negative internal electric field. Moreover, the origin of the polarity change of TPC is also different with that of TPV. It has been indicated that the polarity change was caused by the competition between the negative voltage due to charges generated at the interface and positive one induced by the build-in potential [5,6]. As the case for TPC, however, a polarity change is presented even there is no internal

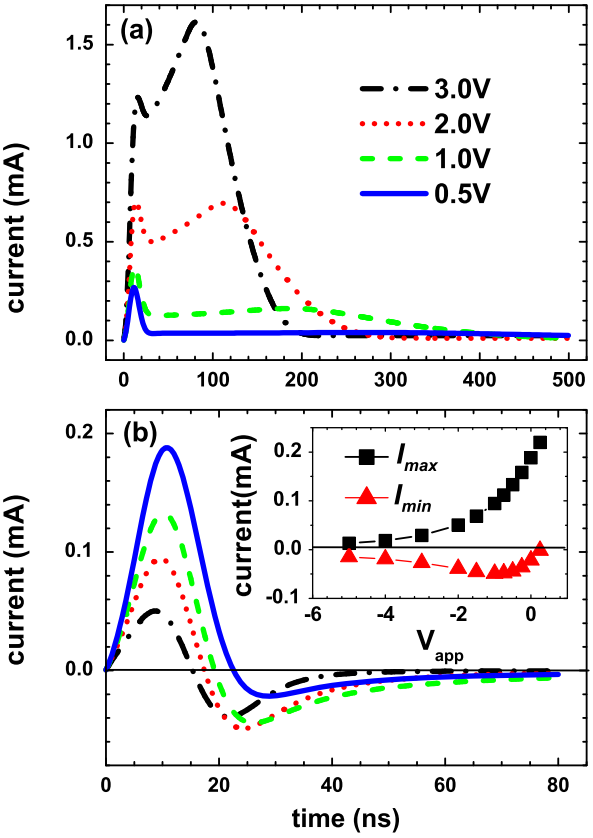

Fig. 5. Transient photocurrent under (a) positive and (b) negative applied voltages. The absolute value of the voltages in (b) is the same with that in (a), correspondingly. The inset of (b) shows the maximum and the minimum value of the photocurrent during evolution as a function of applied voltage V_{app}. $\eta_1 = 1000$ ns^{-1}.

electric field. The conclusion is easily seen from the comparison of curve of $\eta_1 = 0.1$ ns^{-1} with the one $\eta_1 = 1$ ns^{-1} and from the curve with 0.5 V applied voltage in the lower plot of Fig. 5, when the internal voltage is counteracted by the applied voltage. The polarity change of TPC is closely related to the competition between the diffusion and recombination of the charge carrier at the interface. Thereupon, TPC more directly reflects the charge processes at the interface and reveals more transient characteristics in comparison with TPV.

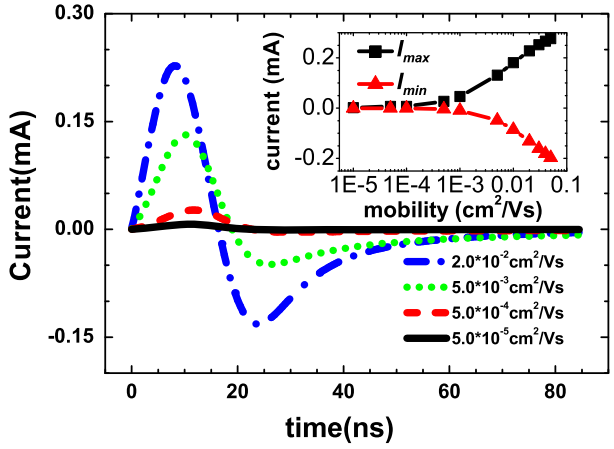

Fig. 6. TPC with different hole mobility μ_p. The inset shows the maximum and the minimum value of the curves as a function of μ_p. $\eta_1 = 1000\ \mathrm{ns}^{-1}$.

TPC is more convenient for investigating the interfacial effects in that the environment of charge carriers in the device can be changed by the applied voltage. In the following, we simulate TPC of devices by changing the external voltage, and the mobility of the organic materials. The results are shown in Fig. 5 and Fig. 6 respectively. As expected, the magnitude of spike increases with increasing voltage. While under large voltage, the platform becomes slope, which is due to drift current accelerated by the large electric field. In Fig. 5(b), the cases of negative applied voltage are shown. Unlike the positive biased voltage condition, the spike is restrained under higher negative voltage. The inset of Fig. 5(b) shows the dependence of the maximum value of the TPC, I_{max}, and the minimum value, I_{min}, on the applied voltage. In Fig. 6, we show the influence of hole's mobility on TPC under negative external voltage, since the TPC is mostly contributed by the diffusion of holes as discussed above. We find that the spike fades away when the mobility is smaller than $1.0 \times 10^{-3}\ \mathrm{cm}^2/\mathrm{V\,s}$. However, it will logarithmically increase with increasing mobility. From this simulation, we realize that the spike could only be observed in the organic material with high enough mobility.

Although the moments, at which the polarity changes of TPV and TPC take place, dependent on the mobility of the material, the applied voltage as well as the exciton interfacial dissociation rate, we pay less attention to them in our simulation due to its complexity. However, we believe that valuable information of charge carrier and exciton processes could be extracted from these time points by further modified simulation and delicate experiments. Besides, we assumed fast exciton dissociation rates and a simple way of exciton dissociation as mentioned above, which also needs further investigation.

4. Summary

In summary, we have investigated the influence of exciton interfacial dissociation on the transient photocurrent by a modified time-dependent device model. The simulation results reveal an essential role of exciton interfacial dissociation on the TPC spike. The spike depends a lot on the applied electric field as well as the mobility of the organic semiconductor. We suggest measuring the favorable TPC of a device with high hole's mobility and with an external voltage that could counteract the build-in potential.

Acknowledgements

The authors would like to acknowledge the financial support from the National Natural Science Foundation of China and the National Basic Research Program of China (2012CB921401 and 2009CB929204).

References

[1] C.W. Tang, S.A. VanSlyke, Appl. Phys. Lett. 51 (1987) 913.
[2] B.A. Gregg, J. Phys. Chem. B 107 (2003) 4688.
[3] T. Dekorsy, T. Pfeifer, W. Kütt, H. Kurz, Phys. Rev. B 47 (1993) 3842.
[4] B. Mahrov, G. Boschloo, A. Hagfeldt, L. Dloczik, T. Dittrich, Appl. Phys. Lett. 84 (2004) 5455.
[5] Q.L. Song, H.R. Wu, X.M. Ding, X.Y. Hou, F.Y. Li, Z.G. Zhou, Appl. Phys. Lett. 88 (2006) 232101.
[6] Y. Yao, X.Y. Sun, B.F. Ding, D.L. Li, X.Y. Hou, C.Q. Wu, Appl. Phys. Lett. 96 (2010) 203306.
[7] M. Borsenberger, D.S. Weiss, Organic Photoreceptors for Xerography, Marcel Dekker, New York, 1998.
[8] P.M. Borsenberger, L. Pautmeier, R. Richert, H. Bässler, J. Chem. Phys. 94 (1991) 8276.
[9] T. Kreouzis, D. Poplavskyy, S.M. Tuladhar, M. Campoy-Quiles, J. Nelson, A.J. Campbell, D.D.C. Bradley, Phys. Rev. B 73 (2006) 235201.
[10] P. Cusumano, S. Gambino, J. Electron. Matter. 37 (2008) 231.
[11] H. Bässler, Phys. Stat. Sol. B 15 (1993) 201.
[12] J.R. Macdonald, J. Appl. Phys. 46 (1975) 4602.
[13] V.I. Arkhipov, H. Bässler, Phys. Stat. Sol. A 6 (2004) 201.
[14] S. Barth, H. Bässler, H. Rost, H.H. Hörhold, Phys. Rev. B 56 (1997) 3844.
[15] V.I. Arkhipov, P. Heremans, H. Bässler, Appl. Phys. Lett. 82 (2003) 4605.
[16] T. Tsuboi, N. Aljaroudi, Phys. Rev. B 72 (2005) 125109.
[17] R. Richert, L. Pautmeier, H. Bässler, Phys. Rev. Lett. 63 (1989) 547.